Functional Redundancy of Variant and Canonical Histone H3 Lysine 9 Modification in *Drosophila*

Taylor J. R. Penke,* Daniel J. McKay,*,†,‡,§ Brian D. Strahl,*,,†† A. Gregory Matera,*,†,‡,§,†† and Robert J. Duronio*,†,‡,§,††,1**

*Curriculum in Genetics and Molecular Biology, †Integrative Program for Biological and Genome Sciences, ‡Department of Genetics, §Department of Biology, **Department of Biochemistry and Biophysics, and ††Lineberger Comprehensive Cancer Center, The University of North Carolina at Chapel Hill, North Carolina 27599

ABSTRACT Histone post-translational modifications (PTMs) and differential incorporation of variant and canonical histones into chromatin are central modes of epigenetic regulation. Despite similar protein sequences, histone variants are enriched for different suites of PTMs compared to their canonical counterparts. For example, variant histone H3.3 occurs primarily in transcribed regions and is enriched for "active" histone PTMs like Lys9 acetylation (H3.3K9ac), whereas the canonical histone H3 is enriched for Lys9 methylation (H3K9me), which is found in transcriptionally silent heterochromatin. To determine the functions of K9 modification on variant *vs.* canonical H3, we compared the phenotypes caused by engineering $H3.3^{K9R}$ and $H3^{K9R}$ mutant genotypes in *Drosophila melanogaster*. Whereas most $H3.3^{K9R}$, and a small number of $H3^{K9R}$, mutant animals are capable of completing development and do not have substantially altered protein-coding transcriptomes, all $H3.3^{K9R}$ $H3^{K9R}$ combined mutants die soon after embryogenesis and display decreased expression of genes enriched for K9ac. These data suggest that the role of K9ac in gene activation during development can be provided by either H3 or H3.3. Conversely, we found that H3.3K9 is methylated at telomeric transposons and that this mark contributes to repressive chromatin architecture, supporting a role for H3.3 in heterochromatin that is distinct from that of H3. Thus, our genetic and molecular analyses demonstrate that K9 modification of variant and canonical H3 have overlapping roles in development and transcriptional regulation, though to differing extents in euchromatin and heterochromatin.

KEYWORDS *Drosophila*; histone variant; H3; transcription; heterochromatin

DNA interacts with histones and other proteins to establish chromatin environments that affect all DNA-dependent processes. The establishment of chromatin environments is accomplished through multiple mechanisms that collectively comprise the bulk of epigenetic regulation found in eukaryotes. In particular, post-translational modification (PTM) of histones influences DNA/histone interactions and also provides binding sites for recruitment of chromatin modulators that influence gene expression, DNA replication and repair, and chromosome segregation during cell division (Wallrath *et al.* 2014). In addition to histone PTMs, epigenetic regulation is modulated by the type of histone protein deposited onto DNA. There are two major categories of histone proteins: the canonical histones and the closely related histone variants (Talbert and Henikoff 2010, 2017). These two histone categories are distinguished by the timing of their expression during the cell cycle and their mechanism of deposition onto DNA. Canonical histones are encoded by multiple genes (*e.g.*, ~55 in humans and ~500 in flies), organized into clusters that are highly expressed during S-phase of the cell cycle, and are deposited onto DNA by the histone chaperone CAF-1 in a replication-coupled manner (Verreault *et al.* 1996; Marzluff *et al.* 2002; Tagami *et al.* 2004). In contrast, variant histones are typically encoded by one or two genes, are expressed throughout the cell cycle, and can be deposited onto DNA independently of replication by histone chaperones other than CAF-1 (Tagami *et al.* 2004; Henikoff and Ahmad 2005; Szenker *et al.* 2011). Variant histones are often deposited at specific genomic locations and have functions that can differ from canonical histones. For example, two

doi: https://doi.org/10.1534/genetics.117.300480
Manuscript received September 1, 2017; accepted for publication November 10, 2017; published Early Online November 13, 2017.
Supplemental material is available online at www.genetics.org/lookup/suppl/doi:10.1534/genetics.117.300480/-/DC1.
[1]Corresponding author: Integrative Program for Biological and Genome Sciences, CB#7100, The University of North Carolina at Chapel Hill, Campus Box 3280, Chapel Hill, NC 27599. E-mail: duronio@med.unc.edu

histone H2A variants, H2AX and H2A.Z, play critical roles in DNA repair (Scully and Xie 2013; Price and Andrea 2014), and the histone H3 variant CENP-A localizes to centromeres and is essential for kinetochore formation (Blower and Karpen 2001; Mellone and Allshire 2003; Henikoff and Ahmad 2005).

The major histone H3 variant in animal genomes is H3.3, which in both mice and *Drosophila* is encoded by two different genes (*H3.3A* and *H3.3B*) that produce identical proteins. Variant histone H3.3 differs from canonical H3.2 and H3.1 by only four or five amino acids, respectively (Szenker *et al.* 2011). In each case, three of these different amino acids are located in the globular domain of H3.3 and are necessary and sufficient for interaction with the replication-independent chaperones HIRA and ATRX-DAXX (Ahmad and Henikoff 2002; Tagami *et al.* 2004; Goldberg *et al.* 2010; Lewis *et al.* 2010). In H3.2, the only replication-dependent histone in *Drosophila*, the fourth amino acid difference occurs at position 31 in the unstructured N-terminal tail (Szenker *et al.* 2011). Histones H3.2 and H3.1 (collectively hereafter referred to as H3), along with H3.3, are some of the most conserved proteins in all eukaryotes (Malik and Henikoff 2003). The conservation of amino acid differences between H3 and H3.3 during evolution strongly suggests that these proteins perform distinct functions. Indeed, H3.3 and H3 are deposited in different genomic regions in a variety of species (Allis and Wiggins 1984; Mito *et al.* 2005; Schwartz and Ahmad 2005; Tamura *et al.* 2009; Jin *et al.* 2011; Kraushaar *et al.* 2013). Also, the level of enrichment for particular PTMs differs between H3.3 and H3 (McKittrick *et al.* 2004; Hake *et al.* 2006), and H3.3-containing nucleosomes can be less stable than those with H3 (Jin and Felsenfeld 2007; Xu *et al.* 2010). Although the epigenetic PTM signature on variant and canonical H3 histones is distinct, the degree to which particular histone PTMs found on both H3 and H3.3 can compensate for one another is not fully understood. Here, we explore the common and distinct functions of variant and canonical H3K9 function during *Drosophila* development.

H3.3 is associated with transcriptionally active regions of the genome with high nucleosome turnover, consistent with H3.3 being enriched in "activating" histone PTMs and depleted in "repressing" histone PTMs (McKittrick *et al.* 2004; Hake *et al.* 2006). One of the histone PTMs enriched on H3.3 relative to H3 is acetylation of lysine nine (K9ac), a mark associated with accessible chromatin (McKittrick *et al.* 2004; Hake *et al.* 2006). Previous studies have identified K9ac at promoters of genes and in regions of high transcriptional activity (Liang *et al.* 2004; Bernstein *et al.* 2005; Roh *et al.* 2005; Kharchenko *et al.* 2011). Additionally, mutation of H3K9 acetyltransferases results in compromised transcriptional output, suggesting that K9ac contributes to or is a consequence of gene expression activation (Georgakopoulos and Thireos 1992; Kuo *et al.* 1998; Wang *et al.* 1998). Importantly, H3K9 acetyltransferases target other histone residues and have nonhistone substrates as well (Glozak *et al.* 2005; Spange *et al.* 2009), indicating that one cannot deduce the function of K9ac solely by mutation of H3K9 acetyltransferases. For example, whereas mutation of the H3K9 acetyltransferase Rtt109 in budding yeast results in sensitivity to DNA-damaging agents, H3K9R mutants, which cannot be acetylated by Rtt109, are insensitive to DNA-damaging agents (Fillingham *et al.* 2008). Direct investigation of K9ac function *in vivo* therefore requires mutation of H3K9 itself. Previously, we used a *Drosophila* histone gene replacement platform (McKay *et al.* 2015) to generate a canonical $H3^{K9R}$ mutant, and found no significant changes in gene expression at regions of the genome enriched in K9ac (Penke *et al.* 2016). This observation raises the possibility that H3.3K9ac functions in gene regulation and can compensate for the absence of H3K9ac.

H3.3 is also found at transcriptionally inactive, heterochromatic regions of the genome (Goldberg *et al.* 2010; Lewis *et al.* 2010; Wong *et al.* 2010). Heterochromatin is enriched in H3K9 di- and trimethylation (me2/me3), modifications that recruit Heterochromatin Protein 1 (HP1) and are essential for heterochromatin function (Bannister *et al.* 2001; Lachner *et al.* 2001; Nakayama *et al.* 2001; Penke *et al.* 2016). DNA within heterochromatin is composed of repeated sequence elements, many of which are transcriptionally silent and consist of immobile transposons or transposon remnants. Using H3.3 mutants, it was recently demonstrated that H3.3 is essential for the repression of endogenous retroviral elements and that H3.3 can be methylated at lysine nine (Elsässer *et al.* 2015). H3.3K9me3 is also important for heterochromatin formation at mouse telomeres (Udugama *et al.* 2015). These studies did not assess the contribution of canonical H3K9 because strategies for mutating all replication-dependent H3 genes in mammalian cells have not been developed. We recently showed in *Drosophila* that mutation of canonical H3K9 causes defects in heterochromatin formation and transposon repression (Penke *et al.* 2016), similar to phenotypes observed in *Caenorhabditis elegans* in the absence of H3K9 methyltransferases (Zeller *et al.* 2016). In addition, we detected low levels of K9me2/me3 in $H3^{K9R}$ mutants. Combined, these data suggest that methylated H3.3K9 plays a role in heterochromatin formation and can compensate for the absence of canonical H3K9. However, the extent of functional overlap between variant and canonical H3K9 and the intriguing possibility that identical modifications on variant or canonical histones have distinct functions has yet to be fully investigated.

To better understand the functions of H3 and H3.3 and to compare the functions of the variant and canonical H3K9 residues, we used clustered regularly interspaced short palindromic repeats (CRISPR)/Cas9 to generate a variant K9R substitution mutation ($H3.3^{K9R}$) in *Drosophila* and combined this with our previously described canonical $H3^{K9R}$ mutant (Penke *et al.* 2016). By comparing the individual mutant phenotypes of $H3.3^{K9R}$ and $H3^{K9R}$ to the combined $H3.3^{K9R}$ $H3^{K9R}$ mutants using a variety of genomic and cell biological assays, we demonstrate that variant and canonical versions of H3K9 can compensate for each other, although to substantially different extents in euchromatin *vs.* heterochromatin. H3K9 plays a more substantial role than H3.3K9 in heterochromatin

formation and in the repression of transposons, whereas they compensate for each other in controlling euchromatic gene expression, particularly in regions enriched in the activating modification, K9ac.

Materials and Methods

Generation of K9R mutant genotypes

Variant *H3.3*^{K9R} mutants generated by the cross scheme illustrated in Supplemental Material, Figure S1A in File S1 were selected by the absence of GFP fluorescence and/or the presence of straight wings. First instar larvae from the variant and canonical *H3.3*^{K9R} *H3.2*^{K9R} cross described in Figure S1B in File S1 were selected based on the presence of GFP fluorescence. Only larvae that receive the H3^{HWT} or H3^{K9R} transgene will survive embryogenesis, as this transgene provides the only source of canonical histone genes. In Table 2, rows one and two indicate progeny from the cross *yw*; *H3.3*^{2x1}/*CyO*, *twiGFP* × *yw*; *Df(2L)BSC110/CyO*, *twiGFP*. Rows three and four indicate progeny from the cross *H3.3B*^{K9R}; *H3.3*^{2x1}/*CyO*, *twiGFP* × *H3.3B*^{K9R}; *Df(2L)BSC110/CyO*, *twiGFP*. In these crosses, the expected ratio of heterozygous to homozygous *H3.3A*^{2x1} animals is 2:1, as *CyO*, *twiGFP/CyO*, *twiGFP* animals do not eclose as adults.

CRISPR/Cas9 mutagenesis and transgene integration

A single guide RNA targeting *H3.3B* near the K9 residue was inserted into pCFD3 and co-injected with a 2-kb homologous repair template containing the H3.3BK9R substitution (File S2). Constructs were injected into embryos expressing Cas9 from the *nanos* promoter (*nanos-cas9*; Kondo and Ueda 2013). Recovered *H3.3B*^{K9R} alleles were subsequently crossed into *H3.3A* null backgrounds [*H3.3A*^{2x1} over deficiency *Df(2L)BSC110*]. Independent *H3.3B*^{K9R} CRISPR alleles were used to generate *trans*-heterozygous animals for all experiments. To generate *H3.3B* rescue constructs, a 5-kb genomic sequence containing the entire wild-type *H3.3B* transcription unit was PCR amplified from genomic DNA of *nanos-cas9* flies and cloned into pATTB (File S2). Gibson assembly (Gibson *et al.* 2009) using primers containing K9R or K9Q substitutions was used to generate mutated versions of *H3.3B*, and all three constructs were integrated into the 86FB *attP* landing site by ΦC31-mediated recombination.

Immunofluorescence

Salivary gland preparations stained using anti-H3K9me2, anti-H3K9me3, anti-H3K9ac, or anti-HP1a were performed as previously described (Cai *et al.* 2010). Antibody sources and concentrations are included in File S2. First instar larval brains were prepared similarly to imaginal wing disc preparations described in Estella *et al.* (2008).

Western blots

ImageJ densitometry analysis was used to determine K9me2, K9ac, or H3 band intensity (See File S2). Histone modification signal was normalized to corresponding H3 loading control signal. Normalized signals from different titrations of the same genotype were averaged and consequent values were set relative to the wild-type value. This process was completed for two biological replicates for both K9me2 and K9ac.

Sample preparation and sequence data analysis

Formaldehyde Assisted Isolation of Regulatory Elements followed by whole-genome sequencing (FAIRE-seq) and RNA sequencing (RNA-seq) samples were prepared from wandering third instar imaginal wing discs as previously described (McKay and Lieb 2013). Sequencing reads were aligned to the dm6 (6.04) reference genome using Bowtie2 (FAIRE) and TopHat (RNA) default parameters (Langmead and Salzberg 2012; Trapnell *et al.* 2014). FAIRE peaks were called with MACS2 using a shift size of 110 bp and a stringency cutoff of 0.01 (Zhang *et al.* 2008). Transcripts were assembled with Cufflinks (Trapnell *et al.* 2014). Bedtools was used to determine read coverage at peaks and transcripts (Quinlan and Hall 2010) and DESeq2 was used to determine statistical significance ($P < 0.05$) (Love *et al.* 2014). The following modENCODE third instar larval chromatin immunoprecipitation sequencing (ChIP-seq) data sets were used: K9me2 = GSE47260 and K9me3 = GSE47258. K9ac ChIP-seq data from imaginal wings discs was generated by Pérez-Lluch *et al.* (2015) (GSM1363590).

Chromatin state analysis was performed using data from Kharchenko *et al.* (2011), which assigns small regions of the genome into one of nine different chromatin states. FAIRE peaks were classified as one or more chromatin states based on overlap with regions defined by Kharchenko *et al.* (2011). Of all the peaks in a particular chromatin state, we determined the percentage of peaks that had significantly different FAIRE signals in mutant compared to wild-type samples. RNA chromatin state analysis was performed in a similar fashion.

Data availability

See Supplemental Experimental Procedures in File S2 for a detailed description of the methods. Strains are available upon request. Sequencing data are available at the Gene Expression Omnibus under accession number GSE106192.

Results

H3.3^{K9R} mutant animals are viable but sterile

To investigate the role of H3.3K9 in *Drosophila* development and compare it to the role of H3K9, we first generated an H3.3^{K9R} animal by introducing a K9R substitution at the endogenous *H3.3B* locus using CRISPR/Cas9 and then combining recovered *H3.3B*^{K9R} mutant alleles with a previously generated *H3.3A* null allele (H3.3A/B combined genotype denoted hereafter as *H3.3*^{K9R}; see Figure S1A in File S1, Table 1, and Table S1 in File S1 for histone genotype nomenclature) (Sakai *et al.* 2009). These *H3.3*^{K9R} mutants, which contain the full complement of

Table 1 Genotype description of H3.3 and H3 K9R mutants

	Canonical histone genotypes		Variant histone genotypes	
Nomenclature	Endogenous	Transgenic	H3.3B	H3.3A
WT	WT	—	WT	WT
H3.3B^{K9R}	WT	—	K9R	WT
H3.3A^{Null}	WT	—	WT	Δ
H3.3^{K9R}	WT	—	K9R	Δ
H3^{HWT}	Δ	WT	WT	WT
H3^{K9R}	Δ	K9R	WT	WT
H3.3^{K9R} H3^{HWT}	Δ	WT	K9R	Δ
H3.3^{K9R} H3^{K9R}	Δ	K9R	K9R	Δ

See Table S1 in File S1 for full genotypes. WT, wild-type (WT); —, no transgenic histone array; Δ, gene deletion.

Table 2 *H3.3^{K9R}* mutants are viable but sterile

H3.3B	*H3.3A*[a]	Observed	Expected	*P*[b]	Fertile
WT	*Δ/+*	535	535.3	n.s.	Yes
WT	*Δ*	268	267.7	n.s.	Yes
K9R	*Δ/+*	400	438	< 0.005	Yes
K9R	*Δ*	257[c]	219	< 0.005	No[d]

WT, wild-type; n.s., not significant.
[a] *H3.3A^{2x1}* deletion allele.
[b] *P*-value calculated with a χ^2 test.
[c] The higher than expected number of observed *H3.3B^{K9R} H3.3A^{Null}* animals is presumably due to nonspecific detrimental effects caused by the presence of a balancer chromosome in siblings with the *H3.3B^{K9R}* mutation and balancer-derived wild-type *H3.3A*.
[d] Both males and females.

endogenous canonical *H3* genes, eclose as adults at the expected Mendelian ratios (Table 2) and appear morphologically normal. Therefore, canonical H3 can provide all of the H3K9 function during *Drosophila* development. This result is consistent with a previous study that found that flies without any H3.3 protein could be propagated as a stock if canonical H3.2 was expressed from a transgene using the *H3.3B* promoter (Hödl and Basler 2012). Our results are also in-line with a previous report in which *H3.3A* and *H3.3B* null animals containing an *H3.3A^{K9R}* transgene were viable (Sakai *et al.* 2009). However, whereas these *H3.3A^{K9R}* transgenic animals were fertile (Sakai *et al.* 2009), we found that animals with an endogenous *H3.3B^{K9R}* mutation and the same *H3.3A* null allele used by Sakai *et al.* (2009) were sterile. The sterility of our *H3.3^{K9R}* animals was rescued in both males and females by a transgene containing the wild-type *H3.3B* gene ectopically integrated into the genome, suggesting that the relative abundance of H3.3^{K9R} causes sterility (Figure S2 in File S1). We conclude that H3.3K9 plays an essential role during gametogenesis and speculate that different amounts of H3.3^{K9R} histones from *H3.3A* or *H3.3B* promoters may account for the differences between our observations and those of Sakai *et al.* (2009).

H3.3K9 and H3K9 have overlapping functions during development

We previously observed that canonical *H3^{K9R}* mutants could complete development, although 98% of these mutant animals died during larval or pupal stages (Penke *et al.* 2016). We considered the possibility that *H3^{K9R}* mutant animals progressed to late larval or pupal stages of development because of compensation by H3.3K9. We therefore tested whether the *H3.3^{K9R}* genotype would advance the *H3^{K9R}* mutant stage of lethality by observing the development of animals in which the *H3.3^{K9R}* and *H3^{K9R}* mutant genotypes were combined (Figure S1B in File S1, Table 1, and Table S1 in File S1). The *H3^{K9R}* genotype was generated using our previously described histone replacement platform (McKay *et al.* 2015; Penke *et al.* 2016). Briefly, the endogenous array of ~100 canonical histone gene clusters was deleted and replaced with an ectopically located transgene encoding a BAC-based, tandem array of 12 canonical histone gene clusters in which the *H3* genes contain a K9R mutation (Figure S1B in File S1). A 12× tandem array of wild-type, canonical histone genes (denoted histone wild-type or *H3^{HWT}*, Figure S1B in File S1), which fully rescues deletion of the endogenous histone gene array, was used as a control (McKay *et al.* 2015). Similar to the *H3.3^{K9R}* mutants, *H3^{HWT}* animals with the *H3.3^{K9R}* mutant genotype (denoted hereafter as *H3.3^{K9R} H3^{HWT}*; see Figure S1B in File S1 and Table 1) were viable (Table 3). However, only 34.6% of *H3.3^{K9R} H3^{HWT}* progeny eclosed as adults (Table 3), compared to essentially 100% of the *H3.3^{K9R}* genotype that contained the full complement of endogenous, wild-type *H3* genes (Table 2). This result suggests that in the presence of fewer total canonical *H3* gene copies, the *H3.3^{K9R}* mutation is more detrimental. Importantly, animals with the *H3.3^{K9R} H3^{K9R}* combined mutant genotype containing both the variant and canonical K9R mutation were 100% inviable, dying with high penetrance at the first instar larval stage, much earlier than the majority of *H3^{K9R}* mutants. These results demonstrate that H3.3K9 can partially compensate for the absence of H3K9, indicating that H3.3K9 and H3K9 have some redundant functions.

H3K9 PTMs are lost in animals lacking H3.3K9 and H3K9

We previously found that the K9me2/me3 signal in *H3^{K9R}* mutant animals is substantially reduced but not absent. Thus, a possible reason why *H3.3^{K9R} H3^{K9R}* mutants have a more severe developmental defect than *H3^{K9R}* mutants is complete loss of K9me throughout the genome. We therefore assessed K9me2/me3 levels in *H3.3^{K9R}* and *H3.3^{K9R} H3^{K9R}* mutants by immunofluorescence. We first assessed K9me2/me3 levels in salivary gland polytene chromosomes of *H3.3^{K9R}* mutants, with the expectation that if H3.3K9 is methylated the signal will be reduced relative to controls. The salivary gland is a highly polyploid tissue (> 1000C), and the alignment of chromatids in the polytene chromosomes results in easily visible structures that provide information about levels and genomic locations of histone PTMs using immunofluorescence. *H3.3^{K9R}* mutants had lower levels of both K9me2 and K9me3 compared to wild-type controls at the largely heterochromatic chromocenter, demonstrating that H3.3K9 is normally methylated in the pericentric heterochromatin of otherwise wild-type

Table 3 *H3.3^{K9R}* and *H3^{K9R}* mutations are synthetically lethal

	Embryo hatching				Pupate[a]				Eclose			
Genotype	Obs	No.	%	*P*[b]	Obs	No.	%	*P*	Obs	No.	%	*P*
H3^{HWT}	389	450	86.4	—	98	140	70.0	—	88	140	62.9	—
H3^{K9R}	370	480	77.1	< 0.0005	183	285	64.2	< 0.05	3	285	1.1	< 0.0005
H3.3^{K9R} H3^{HWT}	350	465	75.3	< 0.0005	279	462	60.4	< 0.0005	160	462	34.6	< 0.0005
H3.3^{K9R} H3^{K9R}	214	325	65.8	< 0.0005	0	130	0.0	< 0.0005	0	130	0.0	< 0.0005

Obs, observed; No., number; —, P value not determined.

[a] The pupation and eclosion values have an identical number of animals analyzed for each genotype because they were obtained from the same brood of animals, while the embryo hatching values were obtained from independent experiments.

[b] *P*-value calculated with a χ^2 test using *H3^{HWT}* observed values as expected values.

animals (Figure 1, A and B). In support of this result, western blot analysis of salivary glands demonstrated that K9me2 levels were decreased in *H3.3^{K9R}* mutants compared to wild-type controls (Figure 1, D and E).

Because *H3.3^{K9R}* mutants exhibited reduced K9me2/me3 signals at the chromocenter, we next used immunofluorescence to examine localization of HP1a, which binds K9me2/me3. In-line with reduced K9me2/me3 signal, HP1a signal at the chromocenter of H3.3^{K9R} mutants was reduced compared to wild-type controls (Figure 1, A and C). HP1a and H3.3 also both localize to telomeres (Goldberg *et al.* 2010; Lewis *et al.* 2010). We found that HP1a localizes to telomeres in *H3.3^{K9R}* mutants (Figure 1A), as it does in *H3^{K9R}* mutants (Penke *et al.* 2016). These results are consistent with previous observations that HP1 recruitment to telomeres requires telomere-binding proteins (Badugu *et al.* 2003; Raffa *et al.* 2011; Vedelek *et al.* 2015) and not the H3K9 methyltransferase Su(var)3-9 (Perrini *et al.* 2004), suggesting that H3K9me is not required for HP1 recruitment to telomeres.

Because *H3.3^{K9R} H3^{K9R}* combined mutants do not develop to the third instar larval stage, we examined K9me2 levels in first instar larval brains. *H3^{K9R}* mutants (with wild-type variant histones) and *H3.3^{K9R} H3^{HWT}* mutants (with a 12× transgenic complement of wild-type canonical histone genes) each exhibited reduced K9me2 levels by immunofluorescence compared to *H3^{HWT}* controls, consistent with the polytene chromosome data (Figure 2A). In contrast, the *H3.3^{K9R} H3^{K9R}* variant and canonical combined mutant brains had undetectable levels of K9me2 in the vast majority of cells (Figure 2A). These results provide further evidence that H3.3K9 is methylated and that the total amount of K9me is derived from both H3.3 and H3.

Interestingly, a small number of cells in the *H3.3^{K9R} H3^{K9R}* first instar mutant brains retained low levels of K9me2 signal at the chromocenter (arrowheads, Figure 2). Cells with residual K9me2 express ELAV, a pan-neuronal marker, and lack expression of Deadpan and Prospero, markers of proliferating neuroblasts and ganglion mother cells, respectively (circles, Figure S3 in File S1). These data indicate that cells with K9me2-positive chromocenters in *H3.3^{K9R} H3^{K9R}* mutant first instar larval brains are differentiated neurons. We suspect that the K9me2 signal in these cells reflects maternally provided wild-type H3 protein remaining in the genomes of quiescent neurons that differentiated prior to having their maternal H3 fully replaced by zygotically expressed H3K9R mutant histones. A corollary to this conclusion is that the proliferating neuroblasts and their GMC daughters have likely progressed through a sufficient number of S phases, such that replacement of maternal H3 with zygotic H3K9R eliminates detectable K9me2 signal.

We also found that levels of H3K9 acetylation were reduced in both the *H3.3^{K9R}* mutant and the *H3^{K9R}* mutant relative to controls, as determined both by immunofluorescence of salivary gland polytene chromosomes (Figure 3, A and B) and by western blots of salivary gland extracts (Figure 3C). Because a substantial amount of K9ac is placed on H3.3, we considered the possibility that a lack of K9ac was responsible for the fertility defects of *H3.3^{K9R}* mutants and the early lethality of *H3.3^{K9R} H3^{K9R}* mutants. To address this question, we integrated either an H3.3B^{K9}, an H3.3B^{K9R}, or an H3.3B^{K9Q} transgene into the same genomic position to determine if a K9Q acetyl mimic could restore fertility to *H3.3^{K9R}* mutants. Animals with only an *H3.3B^{K9R}* mutation at the endogenous locus (*i.e.*, containing a wild-type *H3.3A* gene) and carrying either an H3.3B^{K9R} or H3.3B^{K9Q} transgene were sterile, precluding us from constructing the genotype to test if these transgenes could rescue the sterility of *H3.3^{K9R}* mutant adults (Figure S2 in File S1). This result suggests that both the H3.3B^{K9R} and H3.3B^{K9Q} transgenes acted dominantly to compromise fertility. Furthermore, these data imply that H3.3B^{K9R} and H3.3B^{K9Q} histones are incorporated into chromatin.

H3.3K9 regulates chromatin organization at the chromocenter, telomeres, and transposons

We next asked if the reduction of K9me2/me3 in *H3.3^{K9R}* mutants affected chromatin organization by cytological examination of salivary gland polytene chromosomes using DAPI staining of DNA. As we found previously in *H3^{K9R}* mutants (Penke *et al.* 2016), in some *H3.3^{K9R}* mutants polytene chromosome spreads, the chromocenter appeared abnormal and not fully condensed (Figure 1F). The cause of this phenotype is unclear but may reflect altered chromatin organization or defects in the underreplication of salivary gland pericentric heterochromatin (Belyaeva *et al.* 1998; Zhimulev *et al.* 2003). Based on their cytology, we binned chromocenters into three categories: organized, moderately organized, and disorganized (Figure 1F). We categorized chromocenters from four genotypes: wild-type (*i.e.*, with the endogenous canonical histone genes), an *H3.3A* null mutant (*H3.3A^{Null}*), an *H3.3B* K9R substitution mutant

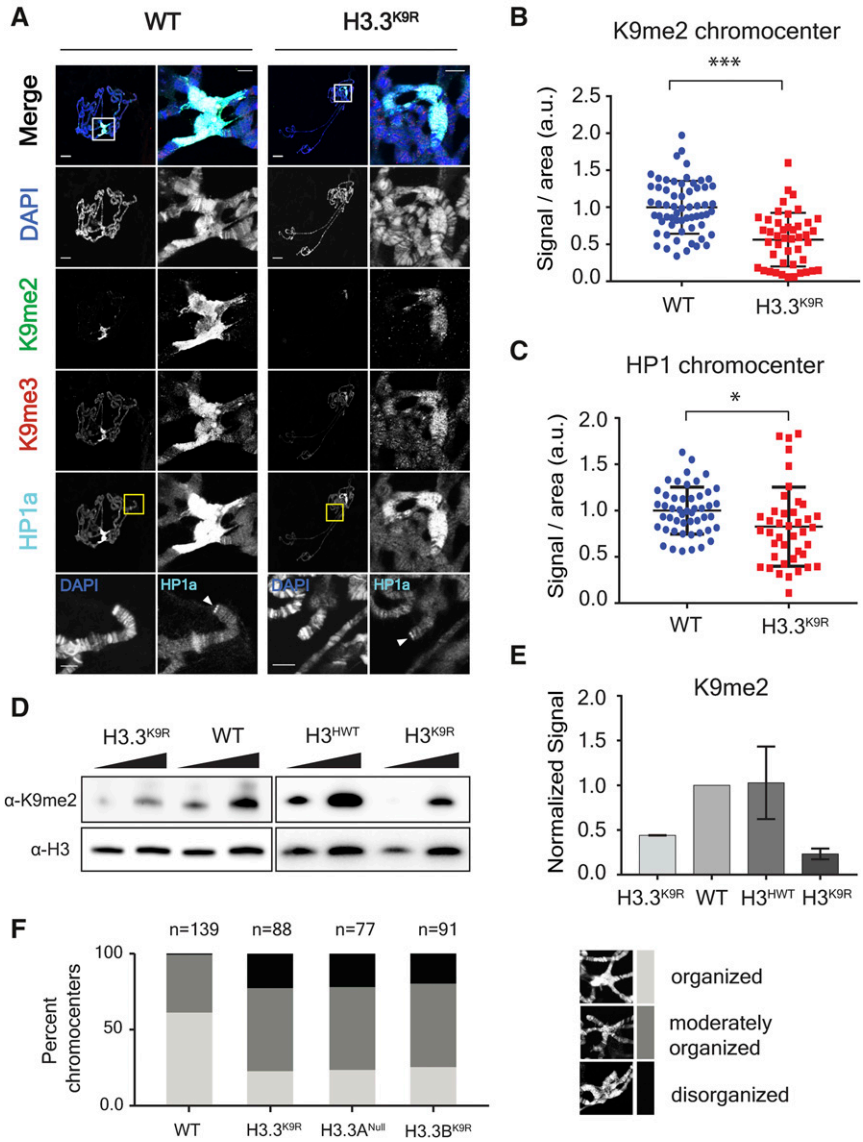

Figure 1 K9me2/me3 and HP1a signal is decreased in H3.3^{K9R} mutants. (A) Third instar larval salivary gland polytene chromosome spreads from wild-type (left) and H3.3^{K9R} mutants (right) stained with anti-K9me2, anti-K9me3, anti-HP1a, and DAPI to mark DNA. Right panel for each genotype shows enlarged chromocenter indicated by white boxes. Bottom panel shows magnified view of telomere indicated by yellow boxes. Bars, 20 μm (whole polytene) and 5 microns (chromocenter/telomere). (B and C) Immunofluorescent signal of K9me2 (B) or HP1a (C) at chromocenters in wild-type (WT) and H3.3^{K9R} mutants (a.u., arbitrary units). Values were normalized to area of the chromocenter and set relative to the average WT value from matched slides (see File S2). Significance was determined using the Student's *t*-test (* $P < 0.05$, ** $P < 0.005$, and *** $P < 0.0005$). (D) Western blot of K9me2 from salivary glands with H3 used as loading control. (E) K9me2 signal was quantified by densitometry and normalized to corresponding H3 loading control band. Normalized values were set relative to WT normalized signal. Error bars represent SEM from two independent biological replicates (see *Materials and Methods*). (F) Quantification of chromocenter organization from *WT*, *H3.3^{K9R}*, *H3.3A^{Null}*, and *H3.3B^{K9R}* mutants.

(*H3.3B^{K9R}*), and the *H3.3B^{K9R}*; *H3.3A^{Null}* double mutant in which all H3.3 contains the K9R substitution (*H3.3^{K9R}*) (Figure S1A in File S1, Table 1, and Table S1 in File S1). Whereas the majority of wild-type chromocenters were organized (60% organized *vs.* 40% moderately organized), both the *H3.3B^{K9R}* and the *H3.3A^{Null}* single mutants had increased percentages of moderately organized and disorganized chromocenters (Figure 1F). For example, ~22% of chromocenters in the various *H3.3* mutants were disorganized compared to < 1% of wild-type chromocenters. These results indicate that H3.3 contributes to chromocenter structure. Interestingly, the *H3.3B^{K9R}*; *H3.3A^{Null}* double mutant had the same proportion of moderately organized and disorganized chromocenters as either single mutant. This result suggests that either reducing *H3.3* gene dose (*i.e.*, the *H3.3A^{Null}* allele) or expressing K9R mutant H3.3 histones (*i.e.*, the *H3.3B^{K9R}* mutation) can prevent normal H3.3 function at pericentric heterochromatin.

Given the disrupted chromocenter structure in *H3.3^{K9R}* mutants, we next examined chromatin structure genome-wide by performing FAIRE-seq. FAIRE-seq provides a measure of local nucleosome occupancy across the genome, revealing regions of "open" chromatin that are relatively depleted of nucleosomes (Simon *et al.* 2013). Using this technique, we previously found that regions of heterochromatin enriched in K9me, particularly pericentromeric heterochromatin, were more open in canonical *H3^{K9R}* mutants relative to *H3^{HWT}* controls (Penke *et al.* 2016). To determine if variant *H3.3^{K9R}* mutants had a similar phenotype, we performed FAIRE-seq in triplicate on imaginal wing discs from wandering third instar larvae in wild-type, *H3.3A^{Null}*, *H3.3B^{K9R}*, and *H3.3B^{K9R}*; *H3.3A^{Null}* (*H3.3^{K9R}*) double mutant genotypes. Sequencing reads were aligned to the genome, and peaks were called on each of the three replicates and combined into a merged peak set. Called peaks were consistent across replicates and read coverage across peaks was highly correlated ($R \geq 0.96$) (Figure S4, A and B in File S1). Additionally, wild-type FAIRE data were consistent with previously generated data from wing discs (McKay and Lieb 2013) (Figure S4D in File S1).

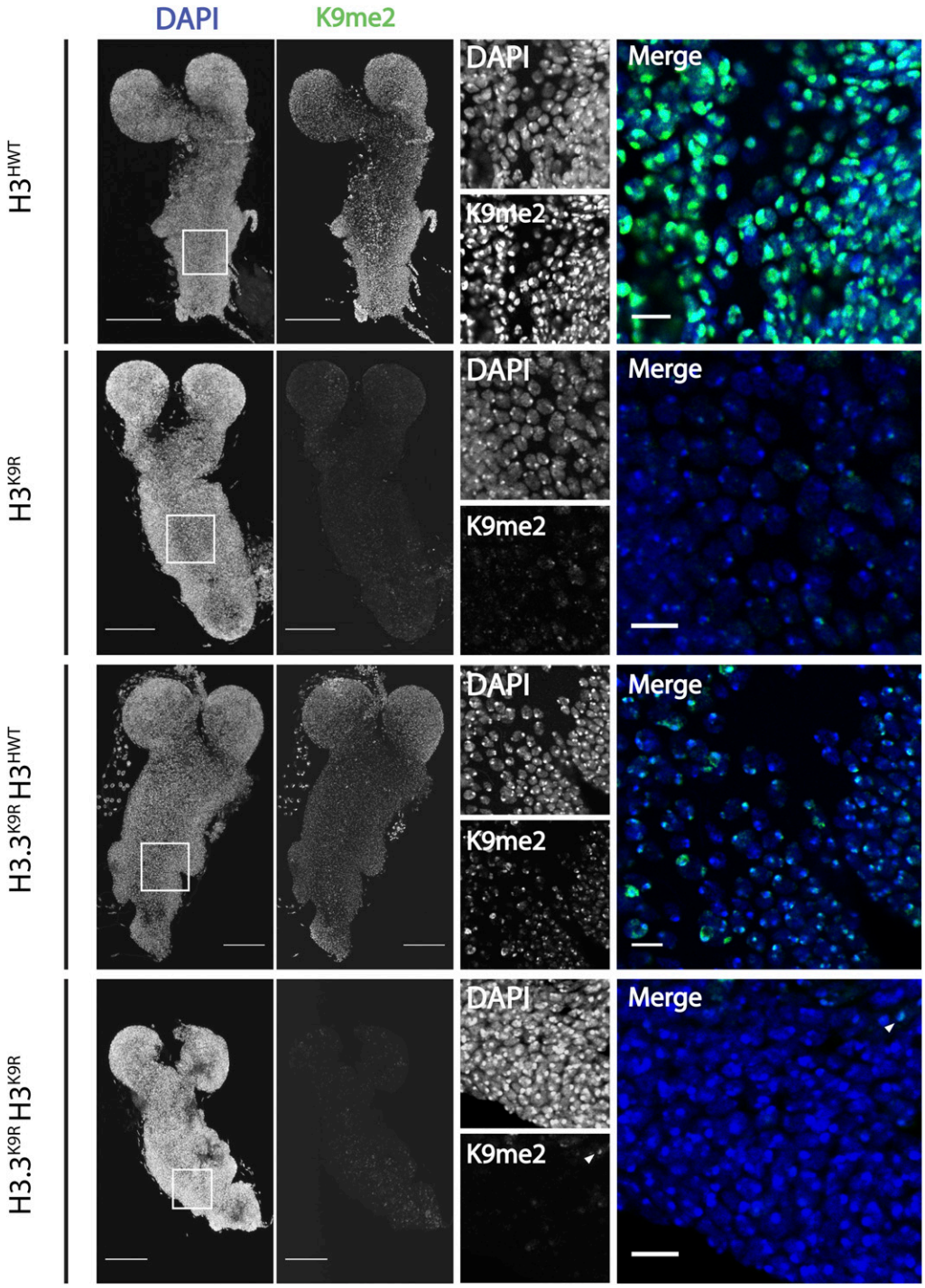

Figure 2 K9me2/me3 signal is diminished in K9R mutants. (A) First instar larval brains stained with anti-K9me2 and DAPI to mark DNA from $H3^{HWT}$, $H3^{K9R}$, $H3.3^{K9R}$ $H3^{HWT}$, and $H3.3^{K9R}$ $H3^{K9R}$ animals. Left panel shows maximum projection of 2-μm confocal sections through the entire brain. Right panel shows a magnified, single confocal section from the area indicated by the white boxes. Arrowheads indicate cells with residual K9me2 signal in $H3.3^{K9R}$ $H3^{K9R}$ animals. Bars, 50 μm (whole brain) and 10 μm (enlarged image).

H3.3A^{Null}, *H3.3B*^{K9R}, and *H3.3*^{K9R} mutants each had a similar percentage of peaks with a significantly altered FAIRE signal when compared to wild-type: 8.8, 6.5, and 7.9%, respectively (Figure 4, A–C). Moreover, significantly changed peaks across the three mutants exhibited a high degree of overlap. Of the 2660 significantly changed peaks across all mutants, 21% were shared among all three and 52% by at least two mutants (Figure S5A in File S1). FAIRE signals at significantly changed peaks also displayed similar fold changes in mutants compared to wild-type and were not exacerbated in the double mutant compared to either single mutant (Figure S5B in File S1). These data suggest that H3.3A and H3.3BK9 both function to regulate chromatin architecture.

We next asked if the changes in FAIRE signals that we observed in *H3.3* mutants were characterized by a particular chromatin signature. We assigned each called FAIRE peak to one of nine different chromatin states characterized by different combinations of histone PTMs, as defined by Kharchenko *et al.* (2011). We then calculated the percentage of FAIRE peaks that changed between an *H3.3* mutant and wild-type within each

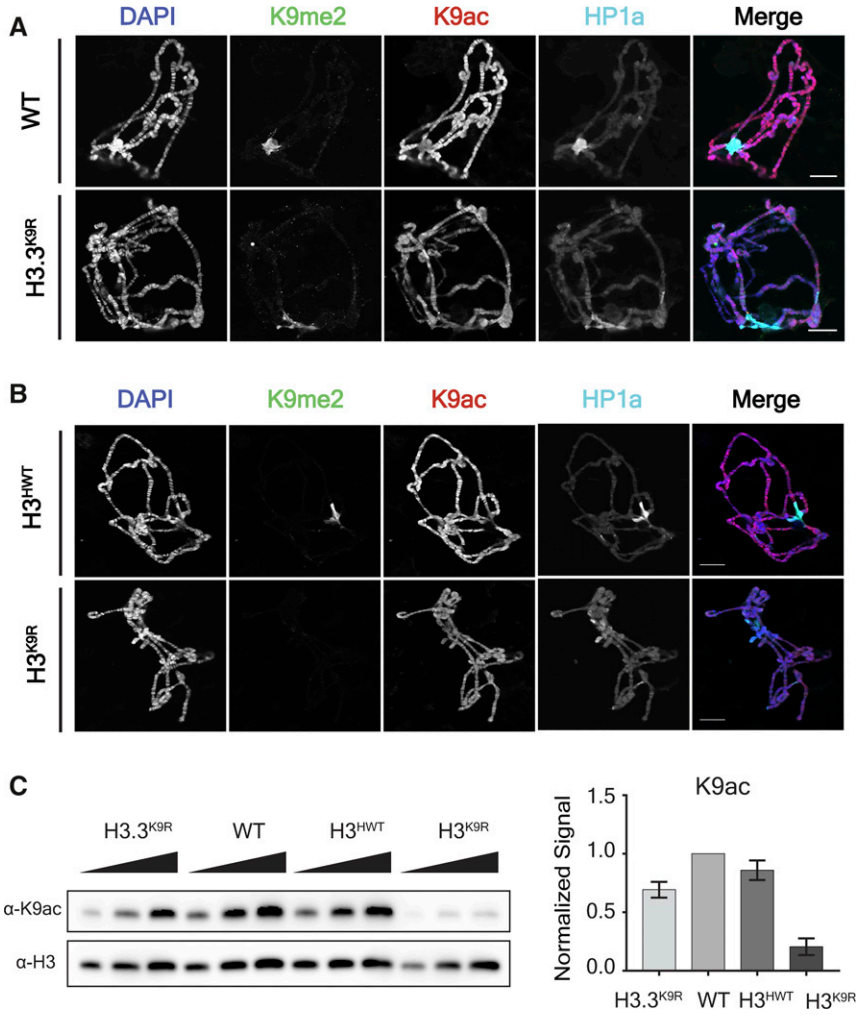

Figure 3 K9ac signal is decreased in H3.3^{K9R} mutants. (A and B) Polytene chromosome spreads from wild-type (WT) and *H3.3*^{K9R} mutants (A) or *H3*^{HWT} and *H3*^{K9R} mutants (B) stained with anti-K9me2, anti-K9ac, anti-HP1a, and DAPI to mark DNA. Bar, 20 μm. (C) Western blot of K9ac from salivary glands with H3 used as loading control. K9ac signal was quantified by densitometry and normalized to corresponding H3 loading control band. Normalized values were set relative to WT normalized signal. Error bars represent SEM from two independent biological replicates (see *Materials and Methods*).

chromatin state. Regions of K9me2/me3 showed the highest percentage of changes in FAIRE signals in *H3.3A*^{Null}, *H3.3B*^{K9R}, and the *H3.3*^{K9R} mutant compared to wild-type, supporting the idea that H3.3K9 is methylated and plays a necessary role in regulating chromatin architecture (Figure 4D). Changes in FAIRE signal was also more likely to occur in regions of H3K36me3, a mark that is enriched along gene bodies that are themselves enriched for H3.3 (Bannister *et al.* 2005; Szenker *et al.* 2011). Finally, we used modENCODE K9me2 and K9me3 ChIP-seq data to complement the chromatin state analysis. Of the FAIRE peaks significantly increased or decreased in *H3.3*^{K9R} mutants compared to wild-type, 76.4% and 49.0% overlapped a K9me2 or K9me3 peak, respectively (Figure 4F). These results demonstrate that altered FAIRE signals in *H3.3*^{K9R} mutants occurred in regions normally occupied by K9me.

We also observed increased FAIRE signal at telomeres in all three *H3.3* mutant genotypes, particularly on chromosomes 2R and 3L (Figure S5C in File S1), suggesting that H3.3 regulates telomeric chromatin architecture. In *Drosophila*, telomeres are composed of retrotransposons enriched in K9me2/me3 (Levis *et al.* 1993; Cenci *et al.* 2005). H3.3 plays a similar role in the mouse, in which H3.3 null mutant embryonic stem cells exhibit an increase in transcripts from transposons (Elsässer *et al.* 2015) and telomeres (Udugama *et al.* 2015). Additionally, we previously observed transposon activation and mobilization in canonical *H3*^{K9R} mutants (Penke *et al.* 2016). For these reasons, we examined FAIRE signal at transposons in our *H3.3* mutants using the piPipes pipeline, which avoids ambiguity in aligning reads to repetitive transposons by mapping to transposon families (Han *et al.* 2015). Both *H3.3A*^{Null} and *H3.3B*^{K9R} mutants resulted in significantly increased FAIRE signal at transposons, and *H3.3*^{K9R} mutants had on average even higher increased FAIRE signal at transposons (Figure 5, A and B). Moreover, FAIRE signal at some telomeric transposons, particularly TART-B, was increased in *H3.3* mutants (Figure 5C). However, the extent of increase in *H3.3*^{K9R} mutants was not as severe as previously observed for *H3*^{K9R} mutants (Penke *et al.* 2016) (Figure 5B). These results support a role for H3.3K9 in chromatin-mediated transposon repression, though to a lesser extent than H3K9.

H3.3K9 and H3K9 functions overlap in regions of K9ac and partially in regions of K9me

To investigate the cause of lethality when both variant and canonical H3 histones contain the K9R mutation, we performed RNA-seq of first instar larvae from four genotypes: *H3*^{HWT},

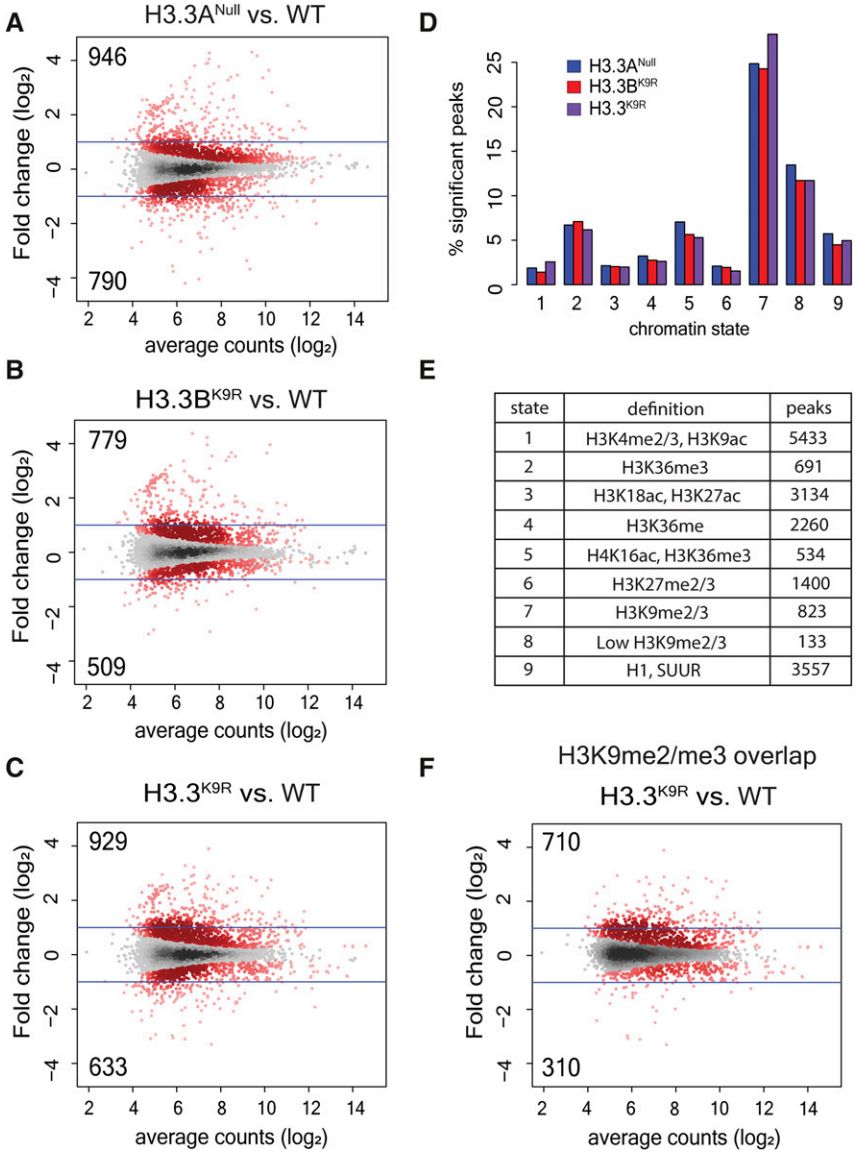

state	definition	peaks
1	H3K4me2/3, H3K9ac	5433
2	H3K36me3	691
3	H3K18ac, H3K27ac	3134
4	H3K36me	2260
5	H4K16ac, H3K36me3	534
6	H3K27me2/3	1400
7	H3K9me2/3	823
8	Low H3K9me2/3	133
9	H1, SUUR	3557

Figure 4 H3.3K9 regulates chromatin architecture in regions of K9me. (A–C) Mutant: wild-type (WT) ratio of *H3.3A*^{null} (A), *H3.3B*^{K9R} (B), or *H3.3*^{K9R} (C). Formaldehyde Assisted Isolation of Regulatory Elements (FAIRE) signal from third instar imaginal wing discs at 19,738 FAIRE peaks called by MACS2. Red dots indicate significantly different peaks ($P < 0.05$), and insets indicate the number of significantly increased (top) or decreased (bottom) peaks. Average counts signify average normalized reads that overlap a peak in mutant and WT samples. (D) Percentage of peaks in a particular chromatin state that have significantly different FAIRE signal in mutants *vs.* WT (top). (E) Summary of histone modifications or proteins that define a chromatin state and the number of FAIRE peaks assigned to a given chromatin state. (F) Plot from (C) showing only those peaks that overlap a K9me2 or K9me3 peak from modENCODE chromatin immunoprecipitation sequencing data.

H3^{K9R}, *H3.3*^{K9R} *H3*^{HWT}, and *H3.3*^{K9R} *H3*^{K9R} (Table 1 and Table S1 in File S1). Larvae of the correct genotype were identified by GFP fluorescence (see *Materials and Methods*). RNA sequencing reads were aligned to the genome using TopHat, transcript assembly was performed by Cufflinks, and DESeq2 was used for statistical analysis (Trapnell *et al.* 2014; Love *et al.* 2014). Each genotype was verified by examination of RNA-seq reads mapping to the K9 codon of variant and canonical histones. Correlation analysis demonstrated that transcript abundance across all assembled transcripts was highly similar among replicates, and was also similar to previously generated data from wild-type first instar larvae (Figure S6 in File S1) (Graveley *et al.* 2011). Additionally, histone expression was similar across all genotypes, suggesting that variation in histone levels does not underlie observed phenotypes (Figure S7A in File S1). In-line with our previous analysis of *H3*^{K9R} RNA-seq data from imaginal wing discs (Penke *et al.* 2016), the majority of significantly changed transcripts in *H3*^{K9R} first instar samples was increased compared to *H3*^{HWT} (247 increased *vs.* 41 decreased), supporting a role for H3K9me in gene silencing (Figure 6A). *H3.3*^{K9R} *H3*^{HWT} samples had a similar number of significantly changed transcripts, and again most transcripts showed increased signals compared to *H3*^{HWT} (203 *vs.* 126), though fold changes were smaller than those of *H3*^{K9R} mutants (Figure 6B). By contrast, the *H3.3*^{K9R} *H3*^{K9R} combined mutant genotype caused a much more pronounced effect on gene expression compared to either the *H3.3*^{K9R} *H3*^{HWT} or the *H3*^{K9R} mutant genotypes (Figure 6C); 869 transcripts exhibited increased RNA signals and 1036 transcripts were decreased compared to *H3*^{HWT} samples. The number of decreased transcripts in *H3.3*^{K9R} *H3*^{K9R} animals compared to *H3*^{HWT} was therefore about 10-fold higher than either the variant or canonical K9R mutant alone. Thus, similar to our viability analysis (Table 3), these RNA-seq results demonstrated that variant and canonical versions of H3K9 compensate for each other in the regulation of gene expression.

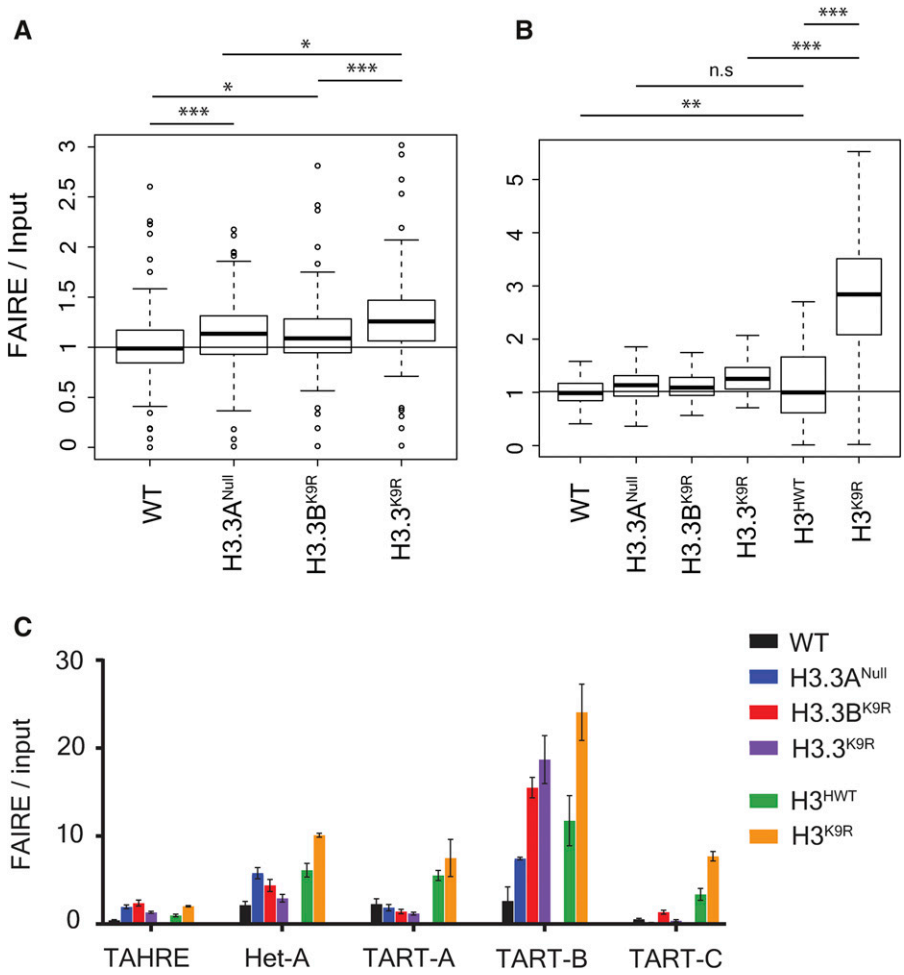

Figure 5 Imaginal wing disc FAIRE signal of *H3.3* mutants is increased at telomeres and transposons. (A) Boxplot of average FAIRE enrichment determined by piPipes pipeline across 126 transposon families (Han *et al.* 2015). Genomic DNA from *Drosophila* embryos used as input control. (B) Boxplots in (A) shown alongside FAIRE enrichment for $H3^{HWT}$ and $H3^{K9R}$ mutants from a separate experiment (Penke *et al.* 2016). (C) FAIRE enrichment of *H3.3* and $H3^{K9R}$ mutants at telomeric transposons. Error bars indicate SD from three replicates for each genotype. Statistical significance determined by paired *t*-test (* $P < 0.05$, ** $P < 0.005$, and *** $P < 0.0005$,). FAIRE, Formaldehyde Assisted Isolation of Regulatory Elements, n.s., not significant; WT, wild-type.

Because we observed increases in FAIRE signal at transposons in $H3.3^{K9R}$ mutants from wing disc samples, we examined RNA levels of transposon families in first instar larvae. Similar to our previous RNA-seq observations from $H3^{K9R}$ mutant wing discs (Penke *et al.* 2016), RNA signal at transposons in $H3^{K9R}$ first instar larvae were increased relative to the $H3^{HWT}$ control (Figure S7, B and C in File S1). Although, on average, transposon levels were only slightly higher in $H3.3^{K9R}$ $H3^{HWT}$ mutants compared to $H3^{HWT}$, transposon levels in $H3.3^{K9R}$ $H3^{K9R}$ combined mutants were significantly higher than either $H3.3^{K9R}$ $H3^{HWT}$ or $H3^{K9R}$ mutants alone (Figure S7, B and C in File S1). Moreover, telomeric transposons are generally increased in all K9R mutants compared to $H3^{HWT}$ controls (Figure S7D in File S1). Together, these results support an overlapping role for H3.3K9 and H3K9 in regulating gene expression and transposon repression.

We next examined chromatin signatures of significantly altered transcripts to explore the mechanism of the observed gene expression changes. All transcripts were assigned to one or more chromatin states based on their overlap with genomic regions defined by Kharchenko *et al.* (2011). We then determined the percentage of transcripts within a given chromatin state that were either increased or decreased in K9R mutants relative to $H3^{HWT}$ controls (Figure 7, A–C). Transcripts in regions of K9me2/me3 (chromatin state 7 and 8) were the most likely to have significantly increased RNA levels in mutants compared to $H3^{HWT}$. Although $H3.3^{K9R}$ $H3^{K9R}$ combined mutants had the highest percentage of chromatin state 7 transcripts that were significantly increased (~26%), $H3^{K9R}$ mutants also displayed a high percentage (~13%) of change within chromatin state 7 (Figure 7, A and D and Figure S8A in File S1). These results suggest that H3.3K9 contributes to gene repression in regions of K9me2/me3 but cannot completely compensate for the absence of H3K9.

In contrast to upregulated transcripts, very few transcripts were significantly decreased in $H3.3^{K9R}$ $H3^{HWT}$ or $H3^{K9R}$ mutants. However, the $H3.3^{K9R}$ $H3^{K9R}$ combined mutant displayed numerous significant decreases in transcript abundance. Interestingly, transcripts in chromatin state 1, characterized by K9ac and a lack of K9me, were most likely to be decreased (Figure 7, B and E). Several other chromatin states showed elevated transcript changes, particularly in the $H3.3^{K9R}$ $H3^{K9R}$ combined mutant; however, in this analysis, transcripts can be assigned to more than one chromatin state. Indeed, many transcripts in chromatin state one also overlap other chromatin states. We therefore performed a supplementary analysis that examined only transcripts that overlap a single

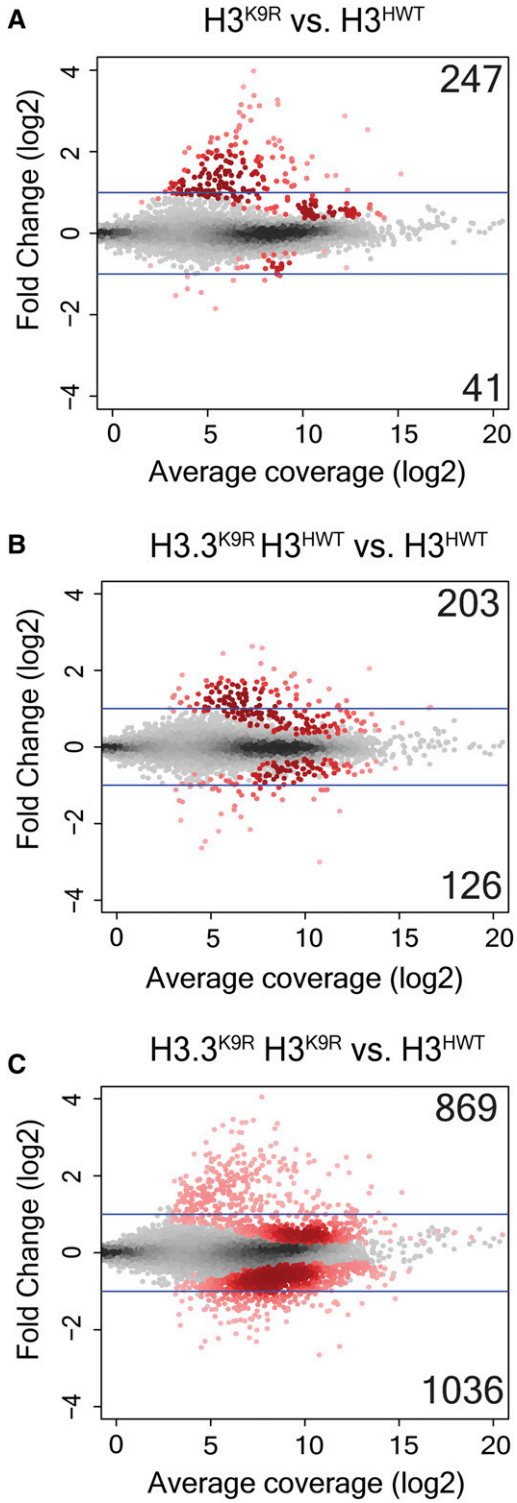

Figure 6 H3.3K9 and H3K9 redundantly regulate gene expression. (A–C) Mutant: wild-type ratio of $H3^{K9R}$ (A), $H3.3^{K9R}$ (B), or $H3.3^{K9R}$ $H3^{K9R}$ (C) RNA signal from first instar larvae at 10,253 transcripts assembled by Cufflinks. The *y*-axis indicates the $\log_2$ transformation of mutant/control signal between the genotypes being compared (indicated at the top of each plot). Red dots indicate significantly different transcripts ($P < 0.05$) and insets signify the number of significantly increased (top) or decreased (bottom) transcripts. Average coverage signifies the average number of normalized reads that overlap a transcript in mutant and $H3^{HWT}$ samples.

chromatin state. This analysis demonstrated that transcripts solely in chromatin state 1 were much more likely to change in K9R mutants than those in other chromatin states (Figure S8A in File S1). Similar results were obtained using imaginal wing disc K9ac ChIP data from Pérez-Lluch *et al.* (2015). Whereas few transcripts that overlapped K9ac were significantly altered in either single mutant (68 in $H3^{K9R}$ and 116 in $H3.3^{K9R}$ $H3^{HWT}$), 1195 K9ac-associated transcripts exhibited changed expression levels in $H3.3^{K9R}$ $H3^{K9R}$ combined mutants (Figure 8). These data suggest that in regions of K9ac, H3.3 and H3 can completely compensate for each other. Additionally, these data provide evidence that K9ac facilitates gene expression.

Discussion

Overlapping and distinct developmental functions of H3 and H3.3

In this study, we determined the distinct and overlapping roles that lysine nine of variant and canonical histone H3 play in gene expression and heterochromatin function during *Drosophila* development. Our developmental genetic analyses demonstrate that H3.3K9 is necessary for fertility but not viability in *Drosophila*. In addition, we find that some euchromatic functions of H3K9 can be provided by either variant H3.3 or canonical H3, whereas H3.3K9 cannot completely compensate for H3K9 in some regions of heterochromatin, as discussed below.

Several studies from multiple species have investigated the developmental functions of H3.3 and H3. In mice, single mutation of either *H3.3A* or *H3.3B* results in reduced viability and compromised fertility (Couldrey *et al.* 1999; Bush *et al.* 2013). Similarly, *Drosophila H3.3A* and *H3.3B* double mutants appear at lower than expected Mendelian ratios and are sterile (Sakai *et al.* 2009). H3.3 in *Tetrahymena thermophila* is also important for sexual reproduction, although it is not required for viability or maintenance of nucleosome density (Cui *et al.* 2006). Both *Tetrahymena* and *Drosophila* H3.3 and H3 can compensate for one another. In *Tetrahymena*, canonical H3 is dispensable if H3.3 is overexpressed (Cui *et al.* 2006). Similarly, in *Drosophila*, transgenic expression of H3 can rescue both the semilethality (Sakai *et al.* 2009) and infertility (Hödl and Basler 2012) of *H3.3* mutants, indicating some functional redundancy between the two histones. Indeed, when expressed equivalently, *Drosophila* H3.3 can provide all of the developmental functions of H3 (Hödl and Basler 2012). Moreover, H3.3 is the sole H3 protein in *Schizosaccharomyces pombe* and *Saccharomyces cerevisiae* yeast (Malik and Henikoff 2003).

H3.3K9 functions in heterochromatin

We find that under endogenous expression conditions, H3.3K9 functions in heterochromatin, including pericentromeric and telomeric regions of the genome. We detected H3.3K9 methylation in pericentromeric heterochromatin,

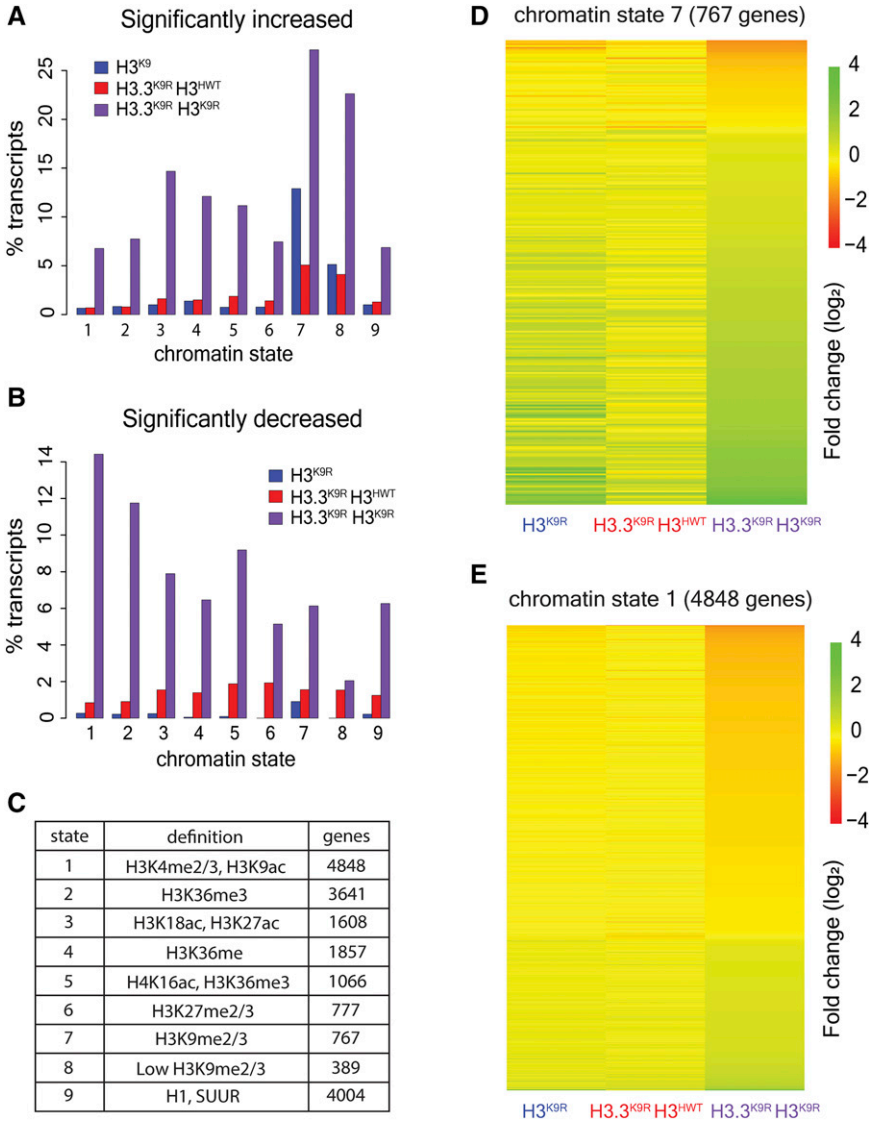

C

state	definition	genes
1	H3K4me2/3, H3K9ac	4848
2	H3K36me3	3641
3	H3K18ac, H3K27ac	1608
4	H3K36me	1857
5	H4K16ac, H3K36me3	1066
6	H3K27me2/3	777
7	H3K9me2/3	767
8	Low H3K9me2/3	389
9	H1, SUUR	4004

Figure 7 H3.3K9 and H3K9 redundancy differs in heterochromatin and euchromatin. (A and B) Percentage of transcripts in a chromatin state that have significantly increased (A) or decreased (B) RNA signal in mutants *vs.* $H3^{HWT}$. (C) Table indicates the number of transcripts that overlap a particular chromatin state. (D and E) Heatmaps showing fold change of K9R mutants over $H3^{HWT}$ at chromatin state 7 regions (D) and chromatin state 1 regions (E). Each row indicates a transcript that overlaps the indicated chromatin state.

congruous with previous data demonstrating that H3.3 in *Drosophila* is deposited at the chromocenter of polytene chromosomes in a replication-dependent manner (Schwartz and Ahmad 2005). We also observed that $H3.3^{K9R}$ mutants exhibited an abnormal chromocenter structure in polytene chromosomes. Moreover, we provide evidence that H3.3K9 is required for the maintenance of telomeric chromatin architecture and repression of certain telomeric transcripts, indicating that replication-coupled expression of H3 cannot provide these particular H3K9 functions. These findings in *Drosophila* are consistent with studies in mouse embryonic stem cells showing that H3.3 is localized to telomeres, is methylated at K9, and functions in the repression of telomeric repeat-containing RNAs (Goldberg *et al.* 2010; Udugama *et al.* 2015). Conversely, the genetic data that we presented here and previously (Penke *et al.* 2016) indicate that H3K9 is essential for the repression of transposon-derived transcripts in pericentric heterochromatin, and that H3.3K9 cannot compensate for the lack of H3K9 at these regions of the genome. The role of H3.3K9 in telomere structure and function may be independent of HP1, as HP1 is recruited to telomeres via the terminin complex independently of H3K9me (Badugu *et al.* 2003; Raffa *et al.* 2011; Vedelek *et al.* 2015).

K9ac regulates euchromatic gene expression

Previous studies that mapped histone modifications across the genome identified K9ac as a characteristic of transcriptionally active regions (Liang *et al.* 2004; Bernstein *et al.* 2005; Roh *et al.* 2005; Kharchenko *et al.* 2011). Moreover, mutation of H3K9 acetyltransferases results in compromised transcriptional activity (Georgakopoulos and Thireos 1992; Kuo *et al.* 1998; Wang *et al.* 1998). However, H3K9 acetyltransferases have nonhistone substrates in addition to H3K9, and decreased transcriptional output may be the result of pleiotropic effects (Glozak *et al.* 2005; Fillingham *et al.* 2008; Spange *et al.* 2009). Our study provides evidence that K9ac, rather than nonhistone targets of H3K9 acetyltransferases, contributes to activating

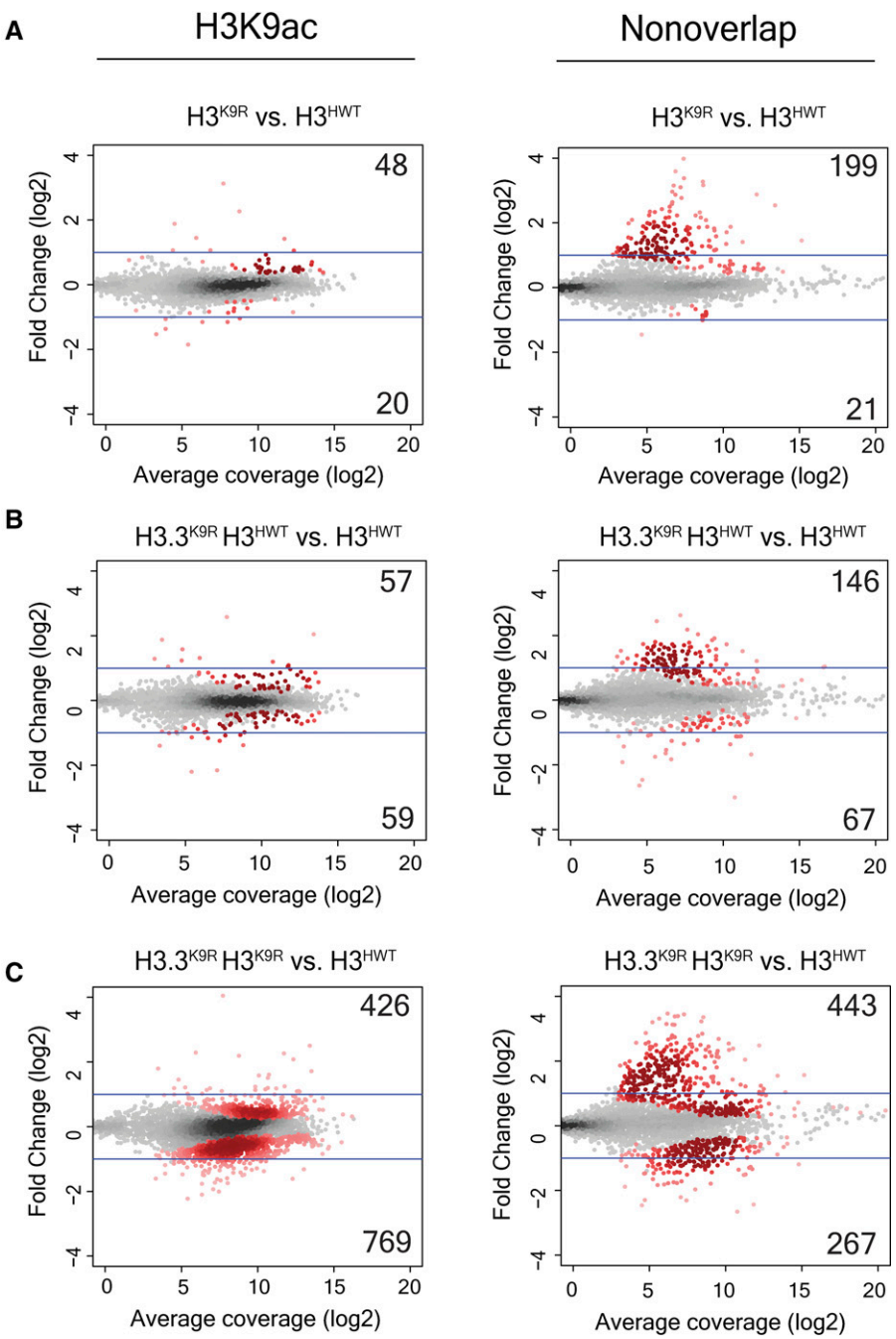

Figure 8 K9ac-associated transcripts are altered in *H3.3*^{K9R} *H3*^{K9R} double mutants. MA (M (log ratio) A (mean average)) plot showing fold change of normalized RNA signal in *H3*^{K9R} (A), *H3.3*^{K9R} *H3*^{HWT} (B), and *H3.3*^{K9R} *H3*^{K9R} (C) mutants *vs. H3*^{HWT} at all transcripts from merged transcriptome. Average coverage on *x*-axis represents the mean expression level of a transcript. Transcripts that overlap a K9ac peak called from chromatin immunoprecipitation sequencing data (GSM1363590; Pérez-Lluch *et al.* 2015) are shown in the left panel, while those that do not are shown in the right panel. Significance (shown in red) was determined using DESeq2 (Love *et al.* 2014) and an adjusted *P*-value cutoff of 0.05.

transcription, as *H3.3*^{K9R} and *H3*^{K9R} mutants exhibit reduced gene expression in regions normally enriched for K9ac. Importantly, these K9ac-rich regions with reduced gene expression are not normally enriched in K9me2 or me3, indicating that the observed phenotype is not due to changes in K9me2 or me3 and likely results from loss of K9ac. This change in gene expression was accompanied by a fully penetrant lethality early in larval development of *H3.3*^{K9R} *H3*^{K9R} combined mutant animals, raising the possibility that gene expression control via acetylation of H3K9 is critical for the completion of animal development. These data are also consistent with previous studies in *C. elegans* demonstrating that H3K9 methylation is not essential for viability (Towbin *et al.* 2012; Zeller *et al.* 2016).

Overlapping and distinct genomic functions of H3K9 and H3.3K9

Functional overlap of H3K9 and H3.3K9 appears to vary at different regions of the genome. Whereas H3.3K9 and H3K9 can perform similar functions in euchromatic regions of the genome and can fully compensate for one another, our RNA-seq data demonstrate that H3.3K9 can only partially compensate for H3K9 in regions of heterochromatin. Partial compensation by H3.3K9 in regions of K9me2/me3

is in-line with previous studies showing that H3.3 is found at heterochromatin (Goldberg *et al.* 2010; Lewis *et al.* 2010; Wong *et al.* 2010) and plays a role in transposon repression (Elsässer *et al.* 2015). In the genotypes that we analyzed, mRNAs encoding variant and canonical H3 are expressed from their native promoters. Thus, disparity in functional overlap might be due to differences in modes of expression and deposition, and thus total amounts of variant and canonical H3 histones in particular regions of the genome. For instance, H3 is normally enriched in heterochromatin compared to H3.3 (Ahmad and Henikoff 2002), which may cause $H3^{K9R}$ mutations to be more detrimental in these regions. However, H3.3 may be able to provide all H3 function when highly expressed in a replication-dependent manner, as a transgenic histone gene array in which the *H3.2* coding region was replaced by *H3.3* is nearly fully functional in larval imaginal discs (Hödl and Basler 2012). Thus, differences in expression and/or deposition into chromatin may be the only basis for functional differences between H3.3 and H3.2 that we observed.

Heterochromatin may be particularly sensitive to the incorporation of nonmodifiable K9 residues. H3K9 methylation serves as a binding site for the protein HP1, which can in turn recruit H3K9 methyltransferases (Grewal and Jia 2007; Elgin and Reuter 2013). Methylation of a neighboring nucleosome can restart the cycle and initiate the propagation of a heterochromatic configuration along the chromosome. The introduction of even a small number of H3K9R-containing nucleosomes may therefore disrupt this cycle, and prevent proper heterochromatin formation and gene repression. Incorporation of $H3.3B^{K9R}$ histones into regions of heterochromatin may dominantly affect chromatin structure, resulting in the observed phenotypes at pericentromeres and telomeres in $H3.3^{K9R}$ mutants. In contrast, incorporation of low amounts of H3K9R histones in euchromatin may not reduce K9ac levels sufficiently to disrupt gene expression. Finally, amino acid differences in variant and canonical H3 may direct distinct histone modification states on different histone types by influencing the binding of chromatin-modifying enzymes (Jacob *et al.* 2014). Different histone modification states on H3.3 and H3 may underlie variation in compensation at different genomic regions.

In summary, our data investigating H3.3K9 and H3K9 function provide evidence that K9ac activates gene expression, and advance our understanding of the overlapping and distinct functional roles of variant and canonical histones.

Acknowledgments

We thank Bhawana Bariar for assistance generating the guide RNA construct, Jeff Sekelsky for the pBlueSurf construct, and Kami Ahmad for providing the $H3.3A^{2x1}$ flies. This work was supported by National Institutes of Health grants 5T32GM007092-39 and F31GM115194 to T.J.R.P. and R01DA036897 to D.J.M., B.D.S., A.G.M., and R.J.D.

Literature Cited

Ahmad, K., and S. Henikoff, 2002 The histone variant H3.3 marks active chromatin by replication-independent nucleosome assembly. Mol. Cell 9: 1191–1200.

Allis, C. D., and J. C. Wiggins, 1984 Histone rearrangements accompany nuclear differentiation and dedifferentiation in Tetrahymena. Dev. Biol. 101: 282–294.

Badugu, R. K., M. M. Shareef, and R. Kellum, 2003 Novel Drosophila heterochromatin protein I (HP1)/origin recognition complex-associated protein (HOAP) repeat motif in HP1/HOAP interactions and chromocenter associations. J. Biol. Chem. 278: 34491–34498.

Bannister, A. J., P. Zegerman, J. F. Partridge, E. A. Miska, J. O. Thomas *et al.*, 2001 Selective recognition of methylated lysine 9 on histone H3 by the HP1 chromo domain. Nature 410: 120–124.

Bannister, A. J., R. Schneider, F. A. Myers, A. W. Thorne, C. Crane-Robinson *et al.*, 2005 Spatial distribution of di- and tri-methyl lysine 36 of histone H3 at active genes. J. Biol. Chem. 280: 17732–17736.

Belyaeva, E. S., I. F. Zhimulev, E. I. Volkova, A. A. Alekseyenko, Y. M. Moshkin *et al.*, 1998 Su(UR)ES: a gene suppressing DNA underreplication in intercalary and pericentric heterochromatin of Drosophila melanogaster polytene chromosomes. Proc. Natl. Acad. Sci. USA 95: 7532–7537.

Bernstein, B. E., M. Kamal, K. Lindblad-Toh, S. Bekiranov, D. K. Bailey *et al.*, 2005 Genomic maps and comparative analysis of histone modifications in human and mouse. Cell 120: 169–181.

Blower, M. D., and G. H. Karpen, 2001 The role of Drosophila CID in kinetochore formation, cell-cycle progression and heterochromatin interactions. Nat. Cell Biol. 3: 730–739.

Bush, K. M., B. T. Yuen, B. L. Barrilleaux, J. W. Riggs, H. O'Geen *et al.*, 2013 Endogenous mammalian histone H3.3 exhibits chromatin-related functions during development. Epigenetics Chromatin 6: 7.

Cai, W., Y. Jin, J. Girton, J. Johansen, and K. M Johansen, 2010 Preparation of Drosophila polytene chromosome squashes for antibody labeling. J. Vis. Exp. 6: 1748.

Cenci, G., L. Ciapponi, and M. Gatti, 2005 The mechanism of telomere protection: a comparison between Drosophila and humans. Chromosoma 114: 135–145.

Couldrey, C., M. B. Carlton, P. M. Nolan, W. H. Colledge, and M. J. Evans, 1999 A retroviral gene trap insertion into the histone 3.3A gene causes partial neonatal lethality, stunted growth, neuromuscular deficits and male sub-fertility in transgenic mice. Hum. Mol. Genet. 8: 2489–2495.

Cui, B., Y. Liu, and M. A. Gorovsky, 2006 Deposition and function of histone H3 variants in Tetrahymena thermophila. Mol. Cell. Biol. 26: 7719–7730.

Elgin, S. C. R., and G. Reuter, 2013 Position-effect variegation, heterochromatin formation, and gene silencing in Drosophila. Cold Spring Harb. Perspect. Biol. 5: a017780.

Elsässer, S. J., K. M. Noh, N. Diaz, C. D. Allis, and L. A. Banaszynski, 2015 Histone H3.3 is required for endogenous retroviral element silencing in embryonic stem cells. Nature 522: 240–244.

Estella, C., D. J. McKay, and R. S. Mann, 2008 Molecular integration of wingless, decapentaplegic, and autoregulatory inputs into distalless during Drosophila leg development. Dev. Cell 14: 86–96.

Fillingham, J., J. Recht, A. C. Silva, B. Suter, A. Emili *et al.*, 2008 Chaperone control of the activity and specificity of the histone H3 acetyltransferase Rtt109. Mol. Cell. Biol. 28: 4342–4353.

Georgakopoulos, T., and G. Thireos, 1992 Two distinct yeast transcriptional activators require the function of the GCN5 protein

to promote normal levels of transcription. EMBO J. 11: 4145–4152.
Gibson, D. G., L. Young, R. Y. Chuang, J. C. Venter, C. A. Hutchison *et al.*, 2009 Enzymatic assembly of DNA molecules up to several hundred kilobases. Nat. Methods 6: 343–345.
Glozak, M. A., N. Sengupta, X. Zhang, and E. Seto, 2005 Acetylation and deacetylation of non-histone proteins. Gene 363: 15–23.
Goldberg, A. D., L. A. Banaszynski, K. Noh, P. W. Lewis, S. J. Elsaesser *et al.*, 2010 Distinct factors control histone at specific genomic regions. Cell 140: 678–691.
Graveley, B. R., A. N. Brooks, J. W. Carlson, M. O. Duff, J. M. Landolin *et al.*, 2011 The developmental transcriptome of Drosophila melanogaster. Nature 471: 473–479.
Grewal, S. I. S., and S. Jia, 2007 Heterochromatin revisited. Nat. Rev. Genet. 8: 35–46.
Hake, S. B., B. A. Garcia, E. M. Duncan, M. Kauer, G. Dellaire *et al.*, 2006 Expression patterns and post-translational modifications associated with mammalian histone H3 variants. J. Biol. Chem. 281: 559–568.
Han, B. W., W. Wang, P. D. Zamore, and Z. Weng, 2015 PiPipes: a set of pipelines for piRNA and transposon analysis via small RNA-seq, RNA-seq, degradome-and CAGE-seq, ChIP-seq and genomic DNA sequencing. Bioinformatics 31: 593–595.
Henikoff, S., and K. Ahmad, 2005 Assembly of variant histones into chromatin. Annu. Rev. Cell Dev. Biol. 21: 133–153.
Hödl, M., and K. Basler, 2012 Transcription in the absence of histone H3.2 and H3K4 methylation. Curr. Biol. 22: 2253–2257.
Jacob, Y., E. Bergamin, M. T. Donoghue, V. Mongeon, C. LeBlanc *et al.*, 2014 Selective methylation of histone H3 variant H3.1 regulates heterochromatin replication. Science 343: 1249–1253.
Jin, C., and G. Felsenfeld, 2007 Nucleosome stability mediated by histone variants H3.3 and H2A.Z. Genes Dev. 21: 1519–1529.
Jin, C., C. Zang, G. Wei, K. Cui, W. Peng *et al.*, 2011 H3.3/H2A.Z double variant-containing nucleosomes mark "nucleosome-free regions" of active promoters and other regulatory regions in the human genome. Nat. Genet. 41: 941–945.
Kharchenko, P., A. Alekseyenko, Y. B. Schwartz, A. Minoda, N. C. Riddle *et al.*, 2011 Comprehensive analysis of the chromatin landscape in Drosophila melanogaster. Nature 471: 480–485.
Kondo, S., and R. Ueda, 2013 Highly improved gene targeting by germline-specific Cas9 expression in Drosophila. Genetics 195: 715–721.
Kraushaar, D. C., W. Jin, A. Maunakea, B. Abraham, M. Ha *et al.*, 2013 Genome-wide incorporation dynamics reveal distinct categories of turnover for the histone variant H3. 3. Genome Biol. 14: 1.
Kuo, M.-H., J. Zhou, P. Jambeck, M. E. A. Churchill, and C. D. Allis, 1998 Histone acetyltransferase activity of yeast Gcn5p is required for the activation of target genes in vivo. Genes Dev. 12: 627–639.
Lachner, M., D. O'Carroll, S. Rea, K. Mechtler, and T. Jenuwein, 2001 Methylation of histone H3 lysine 9 creates a binding site for HP1 proteins. Nature 410: 116–120.
Langmead, B., and S. L. Salzberg, 2012 Fast gapped-read alignment with Bowtie 2. Nat. Methods 9: 357–360.
Levis, R. W., R. Ganesan, K. Houtchens, L. A. Tolar, and F. M. Sheen, 1993 Transposons in place of telomeric repeats at a Drosophila telomere. Cell 75: 1083–1093.
Lewis, P. W., S. J. Elsaesser, K. Noh, S. C. Stadler, and C. D. Allis, 2010 Daxx is an H3.3-specific histone chaperone and cooperates with ATRX in replication-independent chromatin assembly at telomeres. Proc. Natl. Acad. Sci. USA 107: 1–6.
Liang, G., J. C. Y. Lin, V. Wei, C. Yoo, J. C. Cheng *et al.*, 2004 Distinct localization of histone H3 acetylation and H3–K4 methylation to the transcription start sites in the human genome. Proc. Natl. Acad. Sci. USA 101: 7357–7362.
Love, M. I., W. Huber, and S. Anders, 2014 Moderated estimation of fold change and dispersion for RNA-seq data with DESeq2. Genome Biol. 15: 550.
Malik, H. S., and S. Henikoff, 2003 Phylogenomics of the nucleosome. Nat. Struct. Biol. 10: 882–891.
Marzluff, W. F., P. Gongidi, K. R. Woods, J. Jin, and L. J. Maltais, 2002 The human and mouse replication-dependent histone genes. Genomics 80: 487–498.
McKay, D. J., and J. D. Lieb, 2013 A common set of DNA regulatory elements shapes Drosophila appendages. Dev. Cell 27: 306–318.
McKay, D. J., S. Klusza, T. J. R. Penke, M. P. Meers, K. P. Curry *et al.*, 2015 Interrogating the function of metazoan histones using engineered gene clusters. Dev. Cell 32: 373–386.
McKittrick, E., P. R. Gafken, K. Ahmad, and S. Henikoff, 2004 Histone H3.3 is enriched in covalent modifications associated with active chromatin. Proc. Natl. Acad. Sci. USA 101: 1525–1530.
Mellone, B. G., and R. C. Allshire, 2003 Stretching it: putting the CEN(P-A) in centromere. Curr. Opin. Genet. Dev. 13: 191–198.
Mito, Y., J. G. Henikoff, and S. Henikoff, 2005 Genome-scale profiling of histone H3.3 replacement patterns. Nat. Genet. 37: 1090–1097.
Nakayama, J., J. C. Rice, B. D. Strahl, C. D. Allis, and S. I. Grewal, 2001 Role of histone H3 lysine 9 methylation in epigenetic control of heterochromatin assembly. Science 292: 110–113.
Penke, T. J. R., D. J. McKay, B. D. Strahl, A. Gregory Matera, and R. J. Duronio, 2016 Direct interrogation of the role of H3K9 in metazoan heterochromatin function. Genes Dev. 30: 1866–1880.
Pérez-Lluch, S., E. Blanco, H. Tilgner, J. Curado, M. Ruiz-Romero *et al.*, 2015 Absence of canonical marks of active chromatin in developmentally regulated genes. Nat. Genet. 47: 1158–1167.
Perrini, B., L. Piacentini, L. Fanti, F. Altieri, S. Chichiarelli *et al.*, 2004 HP1 controls telomere capping, telomere elongation, and telomere silencing by two different mechanisms in Drosophila. Mol. Cell 15: 467–476.
Price, B. D., and A. D. D. Andrea, 2014 Chromatin remodeling at DNA double strand breaks. Cell 152: 1344–1354.
Quinlan, A. R., and I. M. Hall, 2010 BEDTools : a flexible suite of utilities for comparing genomic features. Bioinformatics 26: 841–842.
Raffa, G. D., L. Ciapponi, G. Cenci, and M. Gatti, 2011 Terminin: a protein complex that mediates epigenetic maintenance of Drosophila telomeres. Nucleus 2: 383–391.
Roh, T., S. Cuddapah, and K. Zhao, 2005 Active chromatin domains are defined by acetylation islands revealed by genome-wide mapping. Genes Dev. 19: 542–552.
Sakai, A., B. E. Schwartz, S. Goldstein, and K. Ahmad, 2009 Transcriptional and developmental functions of the H3.3 histone variant in Drosophila. Curr. Biol. 19: 1816–1820.
Schwartz, B. E., and K. Ahmad, 2005 Transcriptional activation triggers deposition and removal of the histone variant H3. 3. Genes Dev. 19: 804–814.
Scully, R., and A. Xie, 2013 Double strand break repair functions of histone H2AX. Mutat. Res. 750: 5–14.
Simon, J. M., P. G. Giresi, I. J. Davis, and J. D. Lieb, 2013 A detailed protocol for formaldehyde-assisted isolation of regulatory elements (FAIRE). Curr Protoc Mol Biol. 102: 21.26.1–21.26.15.
Spange, S., T. Wagner, T. Heinzel, and O. H. Krämer, 2009 Acetylation of non-histone proteins modulates cellular signalling at multiple levels. Int. J. Biochem. Cell Biol. 41: 185–198.
Szenker, E., D. Ray-Gallet, and G. Almouzni, 2011 The double face of the histone variant H3.3. Cell Res. 21: 421–434.
Tagami, H., D. Ray-Gallet, G. Almouzni, and Y. Nakatani, 2004 Histone H3.1 and H3.3 complexes mediate nucleosome assembly pathways dependent or independent of DNA synthesis. Cell 116: 51–61.
Talbert, P. B., and S. Henikoff, 2010 Histone variants–ancient wrap artists of the epigenome. Nat. Rev. Mol. Cell Biol. 11: 264–275.

Talbert, P. B., and S. Henikoff, 2017 Histone variants on the move: substrates for chromatin dynamics. Nat. Rev. Mol. Cell Biol. 18: 115–126.

Tamura, T., M. Smith, T. Kanno, H. Dasenbrock, A. Nishiyama *et al.*, 2009 Inducible deposition of the histone variant H3.3 in interferon-stimulated genes. J. Biol. Chem. 284: 12217–12225.

Towbin, B. D., C. González-Aguilera, R. Sack, D. Gaidatzis, V. Kalck *et al.*, 2012 Step-wise methylation of histone H3K9 positions heterochromatin at the nuclear periphery. Cell 150: 934–947.

Trapnell, C., A. Roberts, L. Goff, G. Pertea, D. Kim *et al.*, 2014 Differential gene and transcript expression analysis of RNA-seq experiments with TopHat and Cufflinks. Nat. Protoc. 7: 562–578.

Udugama, M., F. T. M Chang, F. L. Chan, M. C. Tang, H. A. Pickett *et al.*, 2015 Histone variant H3.3 provides the heterochromatic H3 lysine 9 tri-methylation mark at telomeres. Nucleic Acids Res. 43: 10227–10237.

Vedelek, B., A. Blastyák, and I. M. Boros, 2015 Cross-species interaction between rapidly evolving telomere-specific drosophila proteins. PLoS One 10: 1–16.

Verreault, A., P. D. Kaufman, R. Kobayashi, and B. Stillman, 1996 Nucleosome assembly by a complex of CAF-1 and acetylated histones H3/H4. Cell 87: 95–104.

Wallrath, L. L., M. W. Vitalini, and S. C. R Elgin, 2014 pp. 529–552 in *Fundamentals of Chromatin*, edited by J. L. Workman and S. M. Abmayr. Springer-Verlag, New York.

Wang, L., L. Liu, and S. L. Berger, 1998 Critical residues for histone acetylation by Gcn5, functioning in Ada and SAGA complexes, are also required for transcriptional function in vivo. Genes Dev. 12: 640–653.

Wong, L. H., J. D. McGhie, M. Sim, M. A. Anderson, S. Ahn *et al.*, 2010 ATRX interacts with H3.3 in maintaining telomere structural integrity in pluripotent embryonic stem cells. Genome Res. 20: 351–360.

Xu, M., C. Long, X. Chen, C. Huang, S. Chen *et al.*, 2010 Partitioning of histone H3–H4 tetramers during DNA replication-dependent chromatin assembly. Science 328: 94–98.

Zeller, P., J. Padeken, R. Van Schendel, V. Kalck, M. Tijsterman *et al.*, 2016 Histone H3K9 methylation is dispensable for Caenorhabditis elegans development but suppresses RNA: DNA hybrid-associated repeat instability. Nat. Genet. 48: 1385–1395.

Zhang, Y., T. Liu, C. A. Meyer, J. Eeckhoute, D. S. Johnson *et al.*, 2008 Model-based analysis of ChIP-Seq (MACS). Genome Biol. 9: R137.

Zhimulev, I. F., E. S. Belyaeva, V. F. Semeshin, V. V. Shloma, I. V. Makunin *et al.*, 2003 Overexpression of the SuUR gene induces reversible modifications at pericentric, telomeric and intercalary heterochromatin of Drosophila melanogaster polytene chromosomes. J. Cell Sci. 116: 169–176.

Communicating editor: P. Geyer